Analysis of Blocking Probability for First-Fit Wavelength Assignment in Transmission-Impaired Optical Networks

Jun He, Maïté Brandt-Pearce, and Suresh Subramaniam

***Abstract*—The quality of an optical signal degrades due to physical layer impairments as it propagates from a transmitter to a receiver. As a result, the signal quality at the receiver of a lightpath may not be sufficiently high, leading to increased call blocking. Consequently, an all-optical network's routing and wavelength assignment algorithm must verify the quality of the lightpath before accepting it. In this paper, analytical expressions for the total blocking probability are derived for first-fit wavelength assignment for networks suffering from transmission impairments. The new technique effectively predicts the performance of wavelength selection techniques that consider either a single candidate channel or all channels for quality of transmission compliance. The analysis is also applicable to first-fit algorithms with different static channel orderings.**

***Index Terms*—Analytical modeling; Bit error rate; Crosstalk; First-fit wavelength assignment; Optical switches; Routing and wavelength assignment; Transmission impairments; Wavelength division multiplexing.**

I. INTRODUCTION

Wavelength routed optical networks (WRONs) are being considered as an alternative to more traditional electrically switched optical networks to increase flexibility and throughput [1,2]. All-optical networking eliminates the restrictions incurred by periodic electronic regeneration, as signals remain in the optical domain from end-to-end through a lightpath. The design of such networks presents new challenges because long length paths that occur in optically switched metro or regional transparent networks can be severely affected by physical layer degradations, such as noise and crosstalk. Recently, routing and wavelength assignment (RWA) algorithms specifically designed to predict and avoid these effects have been the subject of extensive research [3–10]. These techniques take into account the quality of transmission (QoT) of the lightpaths as measured by the bit error rate (BER). In this paper, we present an analytical model to compute blocking probabilities (BPs) for RWA algorithms that use a first-fit (FF) wavelength assignment (WA) technique and block calls due to insufficient wavelengths or unsatisfactory QoT in dynamic traffic networks. Computing the BP by simulation, as is typically done, is a time-consuming process. An analytical model is desirable because it is faster and helps network designers understand the operation of their RWA algorithms subject to transmission degradations.

Several analytical models for random-pick (RP) WA with no QoT constraint have been proposed in the literature [11–13]. For example, in [12], a path decomposition technique is proposed, in which a long path is divided into small segments (of two or three links). Then an approximate Markov process is obtained to study each segment separately and the blocking probability (BP) of the long path is computed by appropriately combining the blocking probabilities of the segments.

However, BPs in WRONs for FF WA are harder to analyze [12,13]. The utilization of a layered graph approach, or "wavelength decomposition," is proposed in several papers [14–17]. In [14] link independence is assumed, thereby overestimating BPs, especially in tandem networks [15,17]. In [15], an object independence assumption is made, where the object is a free link or path. In [16], the traffic is modeled as flowing from one layer to the other, and the overflow traffic is modeled as a Bernoulli–Poisson–Pascal (BPP) process. In [17], the author derives an iterative model to calculate the BP for fixed routing in networks with any topology. It assumes wavelength independence and divides the network into layers, one per wavelength. Moment matching and equivalent path methods are used to characterize the overflow traffic. However, these techniques do not account for blocking due to insufficient QoT.

In more recent research [18], an analytical framework for QoT-aware RP WA algorithms is proposed by extending the techniques published in [11,13]. Only QoT blocking due to noise and self-crosstalk, as defined in [3], is considered, with no differentiation between adjacent and non-adjacent wavelengths. This model cannot be adapted to FF WA because it requires that all wavelengths remain statistically equivalent.

In this paper, we propose an analytical model to compute the BPs for FF WA for networks with QoT constraints. The FF WA algorithm has been shown to be more powerful at reducing wavelength BP in networks not susceptible to physical impairments, and has therefore become one of the preferred techniques [9,19]. The analysis presented is a general tool for evaluating the effect of impairments on the BP. The model can be used to include various types of degradations. In this paper

Manuscript received September 14, 2010; revised March 1, 2011; accepted March 4, 2011; published April 18, 2011 (Doc. ID 135097).

Jun He is with the College of Optical Sciences at The University of Arizona, Tucson, Arizona 85721, USA.

Maïté Brandt-Pearce (e-mail: mb-p@virginia.edu) is with the Charles L. Brown Department of Electrical and Computer Engineering, University of Virginia, Charlottesville, Virginia 22904, USA.

Suresh Subramaniam is with the Department of Electrical and Computer Engineering, George Washington University, Washington, DC 20052, USA.

Digital Object Identifier 10.1364/JOCN.3.000411

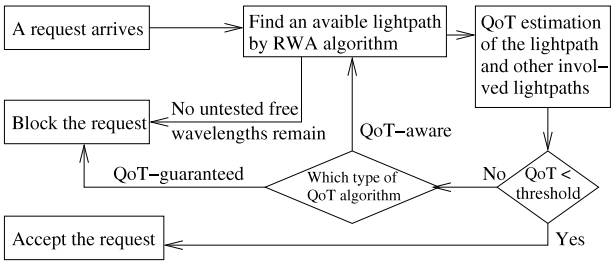

Fig. 1. Flowchart of QoT algorithm incorporating both wavelength blocking and QoT blocking.

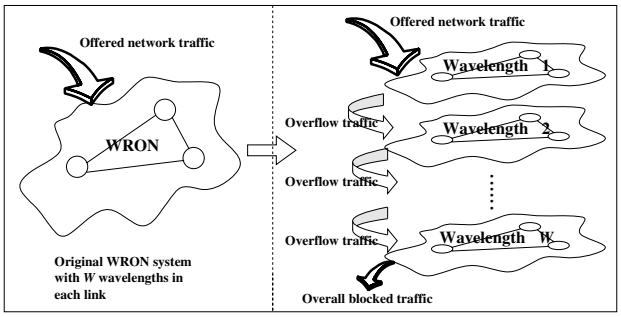

Fig. 2. Layered network model for wavelength-routed optical networks.

we illustrate the use of the general framework by modeling the effect of noise and linear crosstalk.

When adjacent wavelength crosstalk is the primary cause of QoT constraint violations, the FF approach is more vulnerable to physical layer degradations than RP because of FF's successive wavelength usage. Adjacent wavelength crosstalk is due to imperfect WDM demultiplexing, and is significant when the channel spacing is tight compared to the data rates (e.g., 10 Gbps or higher, using a 50 GHz spacing). Even though a state-of-the-art system can be designed to suppress some of the crosstalk, as the throughput increases, the adjacent crosstalk level can be as high as −20 dB, becoming one of the most important sources of physical layer impairment [3]. Hence, it is of great interest to analytically and accurately predict how vulnerable these FF systems are to this type of degradation. Our analytical model can be extended to analyze the impact of other physical impairments on the network performance.

Using our analysis, both wavelength blocking (due to a shortage of a wavelength-continuous lightpath from source to destination) and QoT blocking (due to unacceptable QoT from noise and crosstalk) are included. Each path is treated individually and the total BP is calculated by averaging all path BPs. No wavelength conversion is assumed. The technique can be applied to QoT-guaranteed and QoT-aware FF WA algorithms [8], as shown in Fig. 1. (In a QoT-guaranteed system, as a call request arrives, the RWA chooses a single candidate lightpath using FF and fixed routing and provisions it only if the QoT constraint is satisfied. A QoT-aware algorithm considers multiple lightpaths successively until one is found to satisfy the QoT constraint; if none is found, the call is blocked.) We then apply the technique to an improved FF WA algorithm called *first-fit with ordering* (FFwO), which is shown in [8] to substantially reduce adjacent wavelength crosstalk.

The paper presents our model framework and assumptions in Section II and gives the physical impairments model in Section III. We propose our analytical model that computes the network BP including QoT constraints in Section IV. Several extensions to our analytical model are given in Section V. In Section VI, our analytical techniques are validated using simulation. Conclusions are given in Section VII.

II. Analytical Framework for Computing the BP for FF WA

We develop a method by computing the flow from one layer to another based on QoT blocking as well as wavelength blocking. The QoT blocking is computed by considering all possible network states that create a QoT blocking event, and adding the probability of such states. Which network states cause blocking depends on the type of physical impairment considered.

The WRON with physical impairments is decomposed by wavelengths as a layered system, as shown in Fig. 2. A network with W wavelengths in each link is decomposed into W layered networks, each of which has the same topology but one wavelength capacity in each link. The offered network traffic first goes into layer one, then blocked traffic (overflow traffic) flows down to layer two, and so on. The overflow traffic is modeled as an offered load to the next layer, adjusted for its bursty nature. At layer W, the overflow traffic becomes the overall network blocked traffic, and the BP can be computed. The wavelength continuity constraint, which forces a call to remain on the same wavelength along the path, is automatically enforced in this approach. The probability of each wavelength being used is assumed conditionally independent given the arrival rates. Because this model deals with each wavelength separately and the traffic overflows from one wavelength to the next, it is natural to use this method to analyze FF WA [14–17].

Here we present our assumptions used in the model. The details of our analytical model will be presented in Section IV. We assume that each link between nodes is bidirectional, where each link is actually two fibers, one in each direction and with W wavelengths each. Routing is fixed shortest path and wavelength assignment is FF or FFwO. Y is the set of all source–destination pairs in the network. In general, a route from source node s to destination node d is denoted by $r(s,d)$ or $r(y)$ for $y \in Y$. The notation (s,d) is used when the actual source and destination node values are important; otherwise the equivalent symbol y is employed. Denote the path $r(i,j)$ as a segment of $r(y)$ if it is a subset of $r(y)$. In particular, $r(i,j) \cap r(l,m) = \emptyset$ means that there are no shared links between $r(i,j)$ and $r(l,m)$. An n-hop path $r(0,n)$ is shown in Fig. 3.

Note that a switching and routing operation using a reconfigurable optical add–drop multiplexer (ROADM) based on wavelength selective switching (WSS) technology does not introduce much crosstalk at the nodes. Thus, ROADMs are assumed to not affect the BP due to QoT. We do not count a ROADM node as an additional hop, i.e., only count nodes composed of demultiplexers and multiplexers shown in Fig. 4 as hops. Due to the limitations of ROADM technology, such

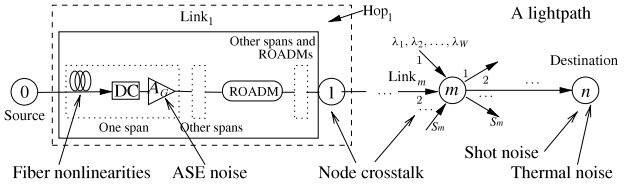

Fig. 3. A generic lightpath structure with $n+1$ nodes and n links. DC is a dispersion compensator. A_G is an in-line optical amplifier. Reconfigurable optical add–drop multiplexers based on wavelength selective switching (WSS) are represented as "ROADM"s.

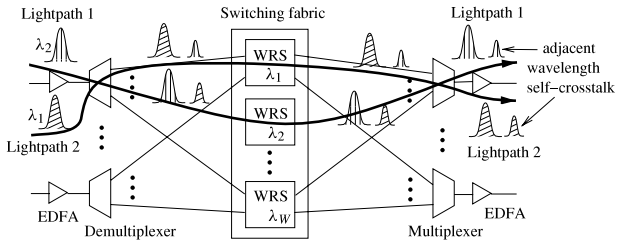

Fig. 4. An all-optical switching node composed of demultiplexers and multiplexers. A WRS is a wavelength-routed switch. Optical add–drop multiplexers (OADMs) are omitted here.

as small number of ports, lightpaths in future networks are likely to consist of several nodes composed of multiplexers and demultiplexers along with ROADM nodes [20].

In Fig. 5 we show one layer of a system. Expressions for the BPs are derived in Section IV. Each layer is divided into two sublayers, a QoT blocking sublayer and a wavelength blocking sublayer. After baseline values for the wavelength BP and flow rates for a QoT-immune system have been computed using the method in Subsection IV.B, the offered traffic is checked for QoT compliance in the QoT blocking sublayer for each path. Then the un-blocked traffic enters the wavelength blocking sublayer and we check whether there is an available lightpath (path and wavelength) to accommodate it. In the QoT-aware case, the total blocked traffic from the two sublayers overflows to the next layer. The QoT BP depends on the usage of other layers and is computed by using the stationary state probabilities in other layers. Thus we have to iterate this process until a steady-state is reached.

In QoT-guaranteed RWA, a part of QoT blocked traffic flows out of the system instead of going to the next layer. Thus, if a call finds an idle path but the QoT is unacceptable, the RWA instantly blocks the call and does not try other wavelengths. We use the probability that an idle lightpath exists for y in the wavelength blocking sublayer to approximate the probability that the y path is idle in the QoT blocking sublayer. Then a proportion of the flow is directly blocked in each layer and removed from the system, i.e., it does not flow to the next layer, which is pictorially represented by the left-pointing arrow in Fig. 5.

Using this framework, we can also evaluate the performance of the FFwO WA algorithm. FFwO was first proposed in [8] to improve the performance of FF WA, which has a low wavelength shortage probability but a high crosstalk level. Based

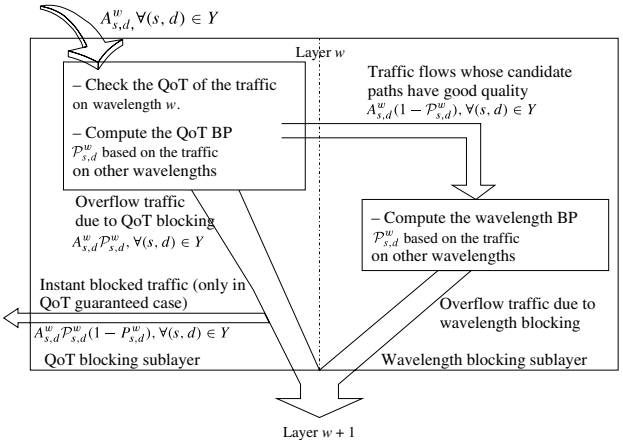

Fig. 5. Flow of analysis of layer w in the layered network model for QoT-aware and QoT-guaranteed WA algorithms.

on the fact that the crosstalk power comes mainly from the adjacent wavelengths, FFwO WA significantly improves the network performance by reordering the wavelength sequence. In FFwO [8], the layer index is not equal to the wavelength index. Thus, for FFwO, in the QoT blocking sublayer we have to choose different layer state probabilities to obtain the QoT blocking, depending on the wavelength ordering. The calculation for wavelength BP is the same as for the FF WA technique. The details are discussed in Section V.

III. Physical Impairments Model

The origins of impairments are highlighted in Fig. 3, which shows a typical lightpath comprising $n+1$ nodes and n links (n hops). Each node is composed of a bank of input and output erbium-doped fiber amplifiers (EDFAs), multiplexers and demultiplexers, and switching fabric, as shown in Fig. 4. Each link can have more than one span. A span contains a long fiber, a dispersion compensator (DC), and an amplifier with gain A_G. Spans could be separated by ROADMs with no effect on our model.

As shown in Fig. 3, the amplified spontaneous emission (ASE) noise accumulates as a signal traverses the spans. In this paper, the power compensation from the EDFA is assumed to be perfect, which means that the signal power is the same at each node and the ASE noise only depends on the number of spans. Thermal and shot noises are both independent of the traffic.

Crosstalk in general can be classified into two categories: one is nonlinear crosstalk, which depends on the nonlinear effects in optical fibers, and the other is linear crosstalk, which occurs in linear WDM components such as demultiplexers and optical switches. Linear crosstalk can be divided into two kinds, out-of-band crosstalk and in-band crosstalk, depending on the wavelength of the crosstalk term [21]. Out-of-band crosstalk is incoherent and is less of a problem since it can be filtered out by optical devices. On the other hand, in-band crosstalk cannot be separated from the desired signal by any optical filter. Thus, in-band node crosstalk is

much more influential in terms of channel performance than out-of-band crosstalk. In this paper, only adjacent wavelength self-crosstalk [3] is considered, which is the in-band crosstalk produced when a leaked copy of the signal follows a different path through an optical cross-connect (OXC) from the input to the output port of the main signal. As shown in Fig. 4, this happens when a lightpath on an adjacent wavelength enters and exits the same OXC ports as the channel of interest. Note that in-band self-crosstalk originates from imperfect WDM demultiplexing and occurs due to an adjacent wavelength's presence. Other types of in-band crosstalk, such as switching crosstalk (due to power leaking in the switching fabric) and neighbor-crosstalk are ignored here; for networks utilizing optical switches based on micro-electro-mechanical systems (MEMS) technology, these two sources of crosstalk are much weaker and are substantially suppressed [22]. Crosstalk due to imperfect WSS in ROADMs is reported to be of the order of −40 dB and therefore also ignorable.

The QoT can be measured by several performance metrics, such as BER of the received signals or other quality measurement metrics [8]. In this work, we assume that the QoT is equivalent to the BER. The BER estimation is based on the physical model used in [8]. Assuming binary on–off keying (OOK) modulation and Gaussian noise, the BER of the signal can be approximated by

$$BER \approx 0.5\ \mathrm{erfc}(Q/\sqrt{2}), \tag{1}$$

where the Q factor is given by [21]

$$Q = \frac{\mu(1)-\mu(0)}{\sigma(1)+\sigma(0)}, \tag{2}$$

where $\mu(k)$ and $\sigma(k)$ are the mean and the standard deviation of the received samples for bit $k \in \{0,1\}$, respectively. The variance can be written as

$$\sigma^2(k) = \sigma^2_{XT}(k) + \sigma^2_{ASE}(k) + \sigma^2_{th} + \sigma^2_{sh}(k), \quad k \in \{0,1\}, \tag{3}$$

where σ^2_{ASE}, σ^2_{th}, and σ^2_{sh} are variances due to ASE noise, thermal noise, and shot noise, respectively, computed as in (6.1.17), (4.4.5), and (4.4.8) of [21]. The crosstalk terms are usually taken to be random and independent of one another, which has been analytically and experimentally validated in [23]. Thus, σ^2_{XT} is determined by the number of adjacent wavelength self-crosstalk components experienced by the lightpath, which can be easily counted as the number of sets of two consecutive hops by the method presented in [24].

Fiber nonlinearities and other physical impairments that depend on the path or on other wavelengths are not considered in this study but could also be incorporated into our approach. For example, in ultra-high capacity systems, such as 40 Gbps and 100 Gbps systems, polarization mode dispersion (PMD) can become important. PMD is a kind of linear impairment related to path length that is caused by differential group delay (DGD) between the principal states of polarization. PMD is a statistical parameter of the system, depending on fiber and environmental conditions [25]. Usually, researchers assign link costs based on DGD of PMD in the routing process [4]. The constrained routing algorithm will find a set of paths that fulfill the requirement of PMD. In our model, we assume that fixed shortest path routing is used to find preset routes. To include the PMD effect, PMD-aware fixed routing can be adopted to find a set of routes. Then we again use our analytical model to capture the behavior of FF WA. The final results would then be an accurate prediction of the BP including the noise, node crosstalk, and PMD.

Four wave mixing (FWM) nonlinear crosstalk may also be included by adding its noise variance σ^2_{NL} to Eq. (3), where σ^2_{NL} can be computed by using the table method proposed in [5], if FWM only has a minor or nominal impact and does not cause QoT blocking on its own. Using the same way of counting the QoT blocking events for node crosstalk, we can incorporate the impact of FWM into the QoT BP calculation. However, if FWM has a dominant impact, the method of QoT event counting proposed in the next section may need to be revised to count QoT blocking caused solely by FWM outside the range of the proposed wavelength matrix for the QoT blocking event. Note that FWM depends on the usage of other wavelengths besides the two most adjacent wavelengths. Accounting for this phenomenon would increase the complexity of the model and could make it prohibitive. Finding a fast approximation for estimating the BP for an FWM-dominant case remains an open problem and is left for future research. Similarly, the incorporation of other impairments such as self- and cross-phase modulation (SPM and XPM) is also left as future work.

IV. RWA Analytical Model With QoT Constraints

In this section, we give a detailed analytical model based on our general analytical framework presented in Section II considering wavelength blocking and QoT blocking due to adjacent wavelength self-crosstalk, ASE noise, thermal noise, and shot noise. Assume lightpaths subject to strong PMD are not considered when fixed paths are pre-computed so that PMD effects are negligible.

We first list the important notation used. Unless otherwise stated, other notions and assumptions are the same as those in Section II.

- W: the total number of accessible wavelengths on the fiber. w is used as the wavelength (layer) index.
- Y: the set of all source–destination pairs in the network, i.e., $Y = \{y_1, \ldots, y_{|Y|}\}$.[1] y without a subscript is used to indicate any source–destination pair (s,d).
- $r(s,d)$ or $r(y)$: a route from source node s to destination node d, i.e., originating from node s and ending at node d.
- Φ_y: the Poisson arrival rate for source–destination pair $y \in Y$.
- $a^w_{i,j}$: the total traffic passing through the segment $r(i,j)$ at layer w, which can be interpreted as the total equivalent Poisson offered load. Note that several paths may pass through the same segment $r(i,j)$. So $a^w_{i,j}$ is the total equivalent Poisson traffic from all (s,d) paths on segment $r(i,j)$ on wavelength w.

[1] We use the notation $|X|$ to denote the cardinality of the set X.

- $\beta_y^w \in \{0,1\}$: the number of currently active calls in $r(y)$ on wavelength (layer) w.
- $A_{s,d}^w$: the equivalent Poisson arrival rate (offered load) to wavelength (layer) w for $r(s,d)$. Then clearly $A_y^1 = \Phi_y$.
- $\bar{A}_y^{w+1}$: the mean value of the overflow traffic from layer w to layer $w+1$. Note that the overflow traffic is not Poisson distributed.
- $\bar{V}_y^{w+1}$: the variance of the overflow traffic from layer w to layer $w+1$.
- $\bar{Z}_y^{w+1}$: the burstiness of the overflow traffic, defined as the ratio of the variance to the mean value.
- P_y^w: the wavelength BP for source–destination pair $y \in Y$ due to wavelength shortage.
- P_y: the overall path wavelength BP for $y \in Y$.
- P: the overall network wavelength BP.
- $N_{\max}(y)$: the maximum number of crosstalk terms allowed in $r(y)$ before the QoT constraint is violated.
- $\underline{I}^w$: a $1 \times |Y|$ random vector, $\underline{I}^w = \left[I_{y_1}^w, \ldots, I_{y_{|Y|}}^w\right]$ for wavelength w, where $I_y^w = 1$ if $r(y)$ is active on wavelength w and $I_y^w = 0$ otherwise.
- $\mathbb{I}^w[y]$: all possible QoT blocking events for source–destination pair y at wavelength (layer) w.
- K: number of blocking events experienced by y, i.e., $K = |\mathbb{I}^w[y]|$.
- $\xi_k^w[y]$: kth QoT blocking event in $\mathbb{I}^w[y]$.
- $\mathscr{P}_y^w$: the QoT BP for $r(y)$ on wavelength w, due to unsatisfactory noise level.
- $\mathbf{P}_y$: the overall BP for path y, including both wavelength blocking and QoT blocking.
- $\mathbf{P}$: the overall network BP.

A. Computing Wavelength BP for a Single Wavelength

Considering an n hop path (see Fig. 3), the state of a wavelength w at time t can be expressed by the $n(n+1)/2$ dimensional process

$$(\beta_{0,1}^w(t), \beta_{0,2}^w(t), \ldots, \beta_{n-1,n}^w(t)), \tag{4}$$

where for $0 \le i < j \le n$ and $0 \le l < m \le n$

$$\beta_{i,j}^w + \beta_{l,m}^w \le 1, \quad \forall r(i,j) \cap r(l,m) \ne 0.$$

The above process is a time-reversible Markov process and the stationary probability vector π^w is given by [26]

$$\pi^w(\beta_{0,1}^w, \beta_{0,2}^w, \ldots, \beta_{n-1,n}^w) = \frac{1}{G_{r(0,n)}^w}\left[(a_{0,1}^w)^{\beta_{0,1}^w} \cdot (a_{0,2}^w)^{\beta_{0,2}^w} \cdots (a_{n-1,n}^w)^{\beta_{n-1,n}^w}\right], \tag{5}$$

where $G_{r(0,n)}^w$ are computed recursively by

$$G_{r(0,n)}^w = G_{r(0,n-1)}^w + \sum_{i=0}^{n-1} G_{r(0,i)}^w a_{i,n}^w, \tag{6}$$

with $G_{r(0,0)}^w = 1$, $w = 1, \ldots, W$ [27]. The equivalent Poisson traffic from all (s,d) paths on segment $r(i,j)$ on wavelength w, $a_{i,j}^w$, is given by [28]

$$a_{i,j}^w = \sum_{\substack{(s,d):r(i,j)\subseteq r(s,d) \\ A_{s,d}^w \text{ assigned uniquely to } (i,j)}} \frac{A_{s,d}^w \cdot (1 - P_{s,d}^w)}{1 - P_{i,j}^w}, \tag{7}$$

where the uniqueness restriction means that if $r(i,j) \leftarrow A_{s,d}^w$ then $r(l,m) \nleftarrow A_{s,d}^w$, $\forall r(l,m) \subseteq r(0,n)$ [17]. The wavelength BP for $r(0,n)$ on wavelength w is computed as

$$P_{0,n}^w = 1 - \pi^w(0,0,\ldots,0) = 1 - \frac{1}{G_{r(0,n)}^w}. \tag{8}$$

B. Computing Wavelength BP for Multiple Wavelengths

We briefly review how the wavelength BP is computed by wavelength decomposition [14–17] in the wavelength blocking sublayer, ignoring QoT blocking. The technique presented here is based on [17].

The traffic blocked on wavelength w flows down to the next wavelength (layer). However, the overflow is not Poisson distributed and its variance is larger than the mean, which indicates that the traffic is bursty [28]. Many studies have analyzed the overflow traffic in conventional circuit switched networks [28]. The mean of the overflow traffic to the next layer is

$$\bar{A}_y^{w+1} = A_y^w \cdot P_y^w. \tag{9}$$

The variance of the overflow traffic $\bar{V}_y^{w+1}$ is computed by using Riordan's formula [28] as

$$\bar{V}_y^{w+1} = \bar{A}_y^{w+1}\left(1 - \bar{A}_y^{w+1} + \frac{\Phi_y}{\bar{\Omega}_y^{w+1} + 1 + \bar{A}_y^{w+1} - \Phi_y}\right), \tag{10}$$

where $\bar{\Omega}_y^w$ is the capacity of an equivalent single-link system for layer 1 to w, which can be obtained from

$$\Phi_y \cdot Er(\Phi_y, \bar{\Omega}_y^{w+1}) = \bar{A}_y^{w+1}. \tag{11}$$

$Er(\Phi_y, \bar{\Omega}_y^w)$ is the generalized Erlang-B formula for non-integral capacity, given as

$$Er(x,y) = \frac{x^y e^{-x}}{\Gamma(y+1)[1 - \Gamma(x, y+1)]}, \tag{12}$$

where $\Gamma(x, y+1)$ is the incomplete Gamma function.

Then the burstiness is defined as the ratio between the variance and the mean value:

$$\bar{Z}_y^{w+1} = \bar{V}_y^{w+1} / \bar{A}_y^{w+1}. \tag{13}$$

Fredericks and Hayward's approximation is used to account for the non-Poisson overflow traffic as [28]

$$A_y^{w+1} \cdot P_y^{w+1} \approx \bar{A}_y^{w+1} \cdot Er\left(\frac{\bar{A}_y^{w+1}}{\bar{Z}_y^{w+1}}, \frac{\Omega_y^{w+1}}{\bar{Z}_y^{w+1}}\right), \tag{14}$$

Algorithm 1 Algorithm to compute the wavelength BP from wavelength w to W given $\bar{A}_y^w$, $\bar{V}_y^w$, and $\bar{Z}_y^w$, $\forall y \in Y$.

1: Assume initial values for $A_y^w = \bar{A}_y^w$, and set the initial path wavelength BP as $P'_y = 0$, $\forall y \in Y$.
2: Compute P_y^w, $\forall y \in Y$ with Eqs. (6), (7), and (8).
3: Calculate the equivalent Poisson traffic A_y^w for layer w with Eqs. (14) and (15), $\forall y \in Y$.
4: **if** $\exists y \in Y$ such that $\frac{\left|P_y^w - P'_y\right|}{P_y^w} > \epsilon$ **then**
5: $P'_y = P_y^w$.
6: Go to Step 2.
7: **else**
8: $w = w + 1$.
9: Compute $\bar{A}_y^w$, $\bar{V}_y^w$, and $\bar{Z}_y^w$ with Eqs. (9), (10), and (11).
10: **if** $w \le W$ **then**
11: Go to Step 1.
12: **else**
13: Calculate path and network wavelength BPs with Eqs. (16) and (17).
14: **return** P and P_y, $\forall y \in Y$.
15: **end if**
16: **end if**

where the value of Ω_y^{w+1} is obtained by

$$P_y^{w+1} = Er(A_y^{w+1}, \Omega_y^{w+1}), \tag{15}$$

and can be treated as the capacity of another equivalent single-link system for only layer $w+1$ with a mean arrival rate of A_y^{w+1}.

Using Eqs. (8) and (14), we can approximate the wavelength BP and path arrival rate for each layer. Then the overall path wavelength BP is computed as

$$P_y = \frac{A_y^W \cdot P_y^W}{\Phi_y} = \frac{\bar{A}_y^{W+1}}{\Phi_y}. \tag{16}$$

The overall network wavelength BP is given by

$$P = \frac{\sum_{y \in Y} \bar{A}_y^{W+1}}{\sum_{y \in Y} \Phi_y}. \tag{17}$$

Algorithm 1 shows the main steps used to compute the overall path and network wavelength BPs for FF WA if $w = 1$, $\bar{A}_y^1 = \Phi_y$, $\bar{V}_y^1 = \Phi_y$, $\bar{Z}_y^1 = 1$, $\forall y \in Y$. If the BPs for two successive iterations differ by less than ϵ for each path, the current layer is deemed stable and the algorithm begins the iteration for the next layer.

C. Counting QoT Blocking Events

To compute the QoT BP, we need to enumerate all possible ways that a QoT blocking event can happen when a call for source–destination pair y reaches wavelength w. Given the network topology, the ASE noise, thermal noise, and shot noise are all determined by the path $r(y)$, $\forall y \in Y$. In our work, the QoT BP depends on the level of noise, the strength of self-crosstalk, and the number of self-crosstalk terms. The number of crosstalk terms for y is the only variable influenced by the instantaneous state of the network. Let $N_{\max}(y)$ represent the maximum number of crosstalk terms allowed in $r(y)$ before the QoT constraint is violated. Using the model for counting the number of crosstalk terms in [24], $N_{\max}(y)$ can be computed for each route $r(y)$, $\forall y \in Y$.

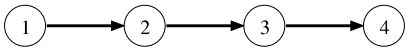

Fig. 6. Topology of a four-node tandem network.

We list all source–destination pairs in Y as $y_1, \ldots, y_{|Y|}$. Random vector $\underline{I}^w$ represents the utilizations of paths at layer w, i.e., the state of the network layer. We use the notation $\underline{I}^w(y') = \left[I_{y_1}^w, \ldots, I_{y'}^w = 1, \ldots, I_{y_{|Y|}}^w\right]$ to represent a state such that path $r(y')$ is known to be used on wavelength w. All used paths on wavelength w form a subset of Y, called $Y^w = \{y : I_y^w = 1\}$. Note that two paths cannot be used in the same layer simultaneously if they share a common link.

According to [3], self-crosstalk happens if and only if two paths share two or more consecutive hops on adjacent wavelengths. One unit of self-crosstalk is introduced to each call for each set of two consecutive hops. If a call is added or dropped at a ROADM, its impact is the same in our model as if it had added or dropped at the next OXC. Given the routing table, we can count how many units of self-crosstalk, say $X_{y'}^y$, are induced by $y \in Y$ on a chosen y' when $r(y)$ is lit on an adjacent wavelength. Define a $1 \times |Y|$ deterministic vector $\underline{X}_{y'} = \left[X_{y'}^{y_1}, \ldots, X_{y'}^{y_{|Y|}}\right]$ describing the crosstalk interference possible at a chosen y' from other source–destination pairs.

Because we consider crosstalk from the nearest adjacent wavelengths only, only lightpaths on wavelength $w-1$ and wavelength $w+1$ can produce crosstalk to $r(y)$ at layer w. Then for a call arriving on y, a QoT blocking event occurs on wavelength w if the current network state at $w-1$ and $w+1$ satisfies

$$(\underline{I}^{w-1} + \underline{I}^{w+1}) \cdot \underline{X}_y^T > N_{\max}(y), \tag{18}$$

where the superscript T indicates a matrix transpose. Furthermore, a newly assigned path on wavelength w must not be allowed to make the QoT of other existing lightpaths violate the QoT requirement. Thus, wavelengths $w+i$ for $i = -2, -1, 0, 1, 2$ have to be considered. Note that we only show equations valid for $w > 2$ and $w < W-2$. For $w = 1, 2, W-1, W$, QoT blocking events that refer to wavelengths outside the spectrum band have to be excluded. To preserve the quality of existing traffic, a call arriving on y has to be blocked if either Eq. (18) holds or

$$\exists y' \in Y^{w+1} \; s.t. \; (\underline{I}^w(y) + \underline{I}^{w+2}) \cdot \underline{X}_{y'}^T > N_{\max}(y') \tag{19}$$

or

$$\exists y' \in Y^{w-1} \; s.t. \; (\underline{I}^w(y) + \underline{I}^{w-2}) \cdot \underline{X}_{y'}^T > N_{\max}(y'). \tag{20}$$

TABLE I
PARAMETER SETTINGS

Parameter	Value
Wavelength spacing	50 GHz
Data rate per channel	10 Gb/s or 40 Gb/s
ASE factor (n_{sp})	1.5
BER threshold	10^{-12} uncoded or 10^{-5} coded
Input EDFA gain	22 dB
Output EDFA gain	16 dB
Center wavelength	1550 nm
Adjacent wavelength crosstalk level	−20 dB
Thermal noise current η_{th}	3.8×10^{-12} A

TABLE II
ROUTING TABLE INCLUDING $N_{\max}$ FOR FIG. 6

Y	y_1	y_2	y_3	y_4	y_5	y_6
(s,d)	(1, 2)	(1, 3)	(1, 4)	(2, 3)	(2, 4)	(3, 4)
$r(s,d)$	(1, 2)	(1, 2, 3)	(1, 2, 3, 4)	(2, 3)	(2, 3, 4)	(3, 4)
$N_{\max}$	2	1	1	2	1	2

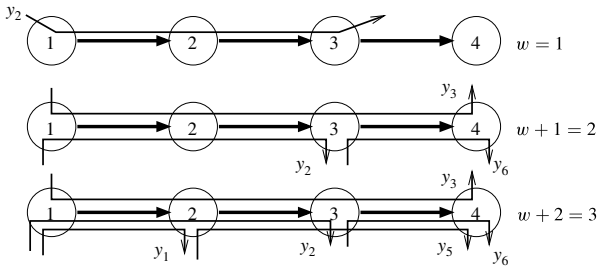

Fig. 7. Possible QoT blocking events of the 2-hop path y_2 on wavelength $w=1$ for the four-node tandem network in Fig. 6. Note that no QoT blocking event is associated with y_4.

Define a $5\times|Y|$ random matrix $\mathbb{I}^w=[\underline{I}^{w-2};\underline{I}^{w-1};\underline{I}^{w};\underline{I}^{w-1};\underline{I}^{w-2}]$, which represents the states in five layers $w+i$ for $i=-2,-1,0,1,2$, centered at layer w. Given a request arriving on y, we can count all possible QoT blocking events, defined by $\mathbb{I}^w[y]=\{\mathbb{I}^w:$ Eqs. (18), (19), or (20) satisfied$\}$ for a call on y. Let $K=\left|\mathbb{I}^w[y]\right|$. Each QoT blocking event is named $\xi_k^w[y]\in\mathbb{I}^w[y]$, $k=1,\ldots,K$.

For example, consider a four-node unidirectional tandem network shown in Fig. 6, with physical layer parameters listed in Table I. The routing table including $N_{\max}$ is shown as Table II. Note that one-hop traffic is not impaired by the self-crosstalk degradation.

We illustrate how the QoT blocking events are counted in the case of a request for the 2-hop path y_2 on wavelength $w=1$ using the FF WA. Based on Eqs. (18), (19), and (20), $\mathbb{I}^w[y_2]$ is composed of all $K=10$ events that create one or more crosstalk terms over the route $r(1,3)$. Assume that wavelength 1 is free along y_2 and the new request is considering occupying wavelength 1 on y_2. If only y_2 on wavelength 2 and wavelength 3 are both occupied, knowing that y_1 on wavelength 1 will be used by the new request, then y_2 on wavelength 1 and 3 will both cause self-crosstalk on wavelength 2. Then the QoT of y_2 on wavelength 2 will not satisfy the requirement because $N(y_2)=2$ is larger than $N_{\max}(y_2)=1$ based on Table II. Then if the incoming request picks wavelength 1 while wavelengths 2 and 3 are occupied by existing traffic, a QoT blocking event will happen. This blocking event can be represented by

$$\xi_1^1[y_2]=\underbrace{\left[\begin{array}{c|c|c|c|c|c}-&-&-&-&-&-\\-&-&-&-&-&-\\*&*&*&*&*&*\\0&1&0&0&0&0\\0&1&0&0&0&0\end{array}\right]}_{y_1\ \ y_2\ \ y_3\ \ y_4\ \ y_5\ \ y_6}\left.\begin{array}{l}w-2=\text{not valid}\\w-1=\text{not valid}\\w=1\\w+1=2\\w+2=3\end{array}\right\}$$

where "−" means that the row is inapplicable because there are no wavelengths less than $w=1$, and "$*$" means that the value is arbitrary, i.e., can be zero or one. Note that $w=1$ has not been assigned to the arriving call; it is just being evaluated for QoT compliance. Other blocking events can be easily enumerated based on Fig. 7. For instance, another blocking event happens if only y_2 and y_6 on wavelength 2 and wavelength 3 are both occupied, which is shown as

$$\xi_2^1[y_2]=\left[\begin{array}{c|c|c|c|c|c}-&-&-&-&-&-\\-&-&-&-&-&-\\*&*&*&*&*&*\\0&1&0&0&0&1\\0&1&0&0&0&1\end{array}\right].$$

Similar to $\xi_1^1[y_2]$ and $\xi_2^1[y_2]$, we list the other eight events in matrix format as follows:

$$\left[\begin{array}{c|c|c|c|c|c}-&-&-&-&-&-\\-&-&-&-&-&-\\*&*&*&*&*&*\\0&1&0&0&0&0\\0&1&0&0&0&1\end{array}\right],\left[\begin{array}{c|c|c|c|c|c}-&-&-&-&-&-\\-&-&-&-&-&-\\*&*&*&*&*&*\\0&1&0&0&0&1\\0&1&0&0&0&0\end{array}\right],$$

$$\left[\begin{array}{c|c|c|c|c|c}-&-&-&-&-&-\\-&-&-&-&-&-\\*&*&*&*&*&*\\0&0&1&0&0&0\\0&1&0&0&0&0\end{array}\right],\left[\begin{array}{c|c|c|c|c|c}-&-&-&-&-&-\\-&-&-&-&-&-\\*&*&*&*&*&*\\0&0&1&0&0&0\\0&1&0&0&0&1\end{array}\right],$$

$$\left[\begin{array}{c|c|c|c|c|c}-&-&-&-&-&-\\-&-&-&-&-&-\\*&*&*&*&*&*\\0&0&1&0&0&0\\0&0&0&0&1&0\end{array}\right],\left[\begin{array}{c|c|c|c|c|c}-&-&-&-&-&-\\-&-&-&-&-&-\\*&*&*&*&*&*\\0&0&1&0&0&0\\1&0&0&0&1&0\end{array}\right],$$

$$\left[\begin{array}{c|c|c|c|c|c}-&-&-&-&-&-\\-&-&-&-&-&-\\*&*&*&*&*&*\\0&1&0&0&0&0\\0&0&1&0&0&0\end{array}\right],\left[\begin{array}{c|c|c|c|c|c}-&-&-&-&-&-\\-&-&-&-&-&-\\*&*&*&*&*&*\\0&1&0&0&0&1\\0&0&1&0&0&0\end{array}\right].$$

D. Computing QoT BP

Because of the wavelength independence assumption, the probability of each event can be directly computed. For example, the probability of the first event described above occurring is given by

$$Pr(\xi_1^1[y_2]) = (1-\mathscr{P}_{y_2}^{w+1})\pi^{w+1}(0,1,0,0,0,0) \times (1-\mathscr{P}_{y_2}^{w+2})\pi^{w+2}(0,1,0,0,0,0). \quad (21)$$

$\pi^{w'}$ is the stationary probability of the state of layer w', as computed by Eq. (5), where its arguments $\beta_{y'}^{w'}$, $y' = 1,\ldots,|Y|$ (from Eq. (4)) are equal to the w' row of the matrix $\xi_i^w[y]$, denoted $\left[\xi_i^w[y]\right]_{w'}$. More generally, we can compute the probability as

$$Pr(\xi_i^w[y]) = \prod_{j=-2}^{-1} \frac{1}{1-Pr(r(y) \text{ idle in } w+j)} \times \prod_{j=-2}^{2} \left[\prod_{y':\left[\xi_i^w[y]\right]_{(w+j,y')}=1} (1-\mathscr{P}_{y'}^{w+j})\pi^{w+j}\left(\left[\xi_i^w[y]\right]_{(w+j)}\right) \right] \quad (22)$$

for $2 < w < W-1$, where $\left[\xi_i^w[y]\right]_{(w',y')}$ is the (w',y') element of the matrix $\xi_i^w[y]$. Note that for layers greater than or equal to w ($j = 0,1$, and 2), the network can be in any state, but, for layers less than w ($j = -1$ and -2), $r(y)$ cannot be idle because y has to have flowed down to w from the upper layer. This is represented by the factor of $Pr(r(y)$ idle in $w+j)$ in Eq. (22) and computed by

$$Pr(r(y) \text{ idle in } w+j) = \frac{1}{G_{r(y)}^{w+j}}. \quad (23)$$

The QoT BP is the sum of the probabilities of the K disjoint blocking events, given by

$$\mathscr{P}_y^w = \sum_{i=1}^{K} Pr(\xi_i^w[y]). \quad (24)$$

Generally K is a large number ($K = 10$ for y_2 in our tiny four-node tandem network). We can decrease the computational complexity of the algorithm by lumping the states together, as more general blocking events. The QoT BP can then be calculated as the probability of the union of these (not disjoint) events. For example, a blocking event will occur if either $w-1$ or $w+1$ have non-zero crosstalk; the probabilities of these events are more easily computed, yet more complex to combine since they are not disjoint.

Networks affected by other types of impairments than additive crosstalk would generate other types of blocking events, but the framework presented here could still be used. An estimate of the probability of the blocking states would need to be derived and combined using Eq. (24).

E. Approximation to Compute QoT Blocking

The complexity of counting all QoT blocking events is only reasonable for small networks and is prohibitive in large networks. We propose an approximation to estimate the QoT BP for large networks with any topology. We observe that the crosstalk mainly originates from the nodes that the considered path passes through. Hence, instead of looking at the whole network, we isolate the considered path, y', to a tandem network with five or fewer wavelength layers that are independent of each other. This isolated tandem network consists of the same hops as y' does. For a candidate wavelength w', the analytical model only considers its related five (including itself) or fewer wavelengths (if $w' = 1,2,W-1$, or W). Sources of crosstalk are modeled as originating from segments of y', instead of considering all source–destination pairs that intersect y'. In the above example, when we compute the QoT BP for y_2, the isolated network becomes a two-hop tandem network consisting of nodes 1, 2, and 3, because y_2 consists of these three nodes. Then K is reduced from 10 to 1 for $w = 1$. The only QoT event is that y_2 itself is used at layers $w+1$ and $w+2$.

Note that the impact of other traffic flows is still included because Eq. (7) in its entirety is still used to compute the arrival rates for this two-hop network. For example, the flow along $r(1,4)$ has been incorporated into $a_{i,j}^w$ in Eq. (7). Since the major part of the crosstalk comes from the links shared with the path being considered, this approximation can include most of the impact of crosstalk, yet with lower complexity. Note that no special algorithms are needed to separate the network. The approximation isolates the selected path into a smaller tandem network and only QoT events that occur in this isolated network are counted. In Section VI, we compare the approximate solution with the exact solution and show it to have accurate results for the four-node tandem network shown in Fig. 6. We also validate the approximate solution via simulation for larger networks.

F. Total BP for QoT-Aware RWA

The total path and network BPs for QoT-aware RWA are computed using Eqs. (16) and (17), where $\bar{A}_y^{W+1}$ now includes the QoT blocking traffic. The detailed steps are shown in Algorithm 2. We obtain the arrival rates and state probabilities in Step 2 for the network without physical impairments, which are used as the initial values in the QoT estimation. Then, the flow proceeds to the QoT blocking sublayer, after which part of the flow with rate

$$\bar{A}_y^w = A_y^w \cdot (1-\mathscr{P}_y^w) \quad (25)$$

returns to the wavelength blocking sublayer. Note that $\bar{A}_y^w$ is not equal to the Poisson traffic rate for the wavelength blocking sublayer; it is the bursty overflow traffic rate whose burstiness is given by Eq. (13). Hence, we obtain the equivalent Poisson arrival rate and BP for this sublayer in Step 4. Then the overflow traffic for layer $w+1$ is equal to the sum of the flow due to QoT blocked calls and wavelength blocked calls, which

Algorithm 2 Algorithm to compute the total blocking for QoT-aware RWA from wavelength $w = 1$ to W given $\bar{A}_y^1 = \Phi_y$, $\bar{V}_y^1 = \Phi_y$, and $\bar{Z}_y^1 = 1 \forall y \in Y$. Set $\mathbf{P}'_y = P_y$.

1: Set $w = 1$.
2: Wavelength blocking sublayer: $\forall y \in Y$, use Algorithm 1 to compute $P_y^{w'}$ and $A_y^{w'}$ for $w' = w$ to W.
3: QoT blocking sublayer: $\forall y \in Y$, compute $\mathscr{P}_y^w$ by Eqs. (22) and (24).
4: Wavelength blocking sublayer: $\forall y \in Y$, recalculate arrival rate $\bar{A}_y^w$ using Eq. (25); obtain $\bar{V}_y^w$, and $\bar{Z}_y^w$ by Eqs. (10) and (11); recalculate P_y^w using Eq. (8); use Eq. (14) to obtain $\hat{A}_y^w$; calculate $\bar{A}_y^{w+1}$ from Eq. (26); update $\bar{V}_y^{w+1}$, and $\bar{Z}_y^{w+1} \forall y \in Y$ by Eq. (10) and (11).
5: Set $w = w + 1$.
6: **if** $w \le W$ **then**
7: Go to Step 2.
8: **else**
9: Calculate $\mathbf{P}_y$ by Eq. (16).
10: **if** $\exists y \in Y$ such that $\frac{|\mathbf{P}_y - \mathbf{P}'_y|}{\mathbf{P}_y} > \epsilon$ **then**
11: $\mathbf{P}'_y = \mathbf{P}_y$. Go to Step 1.
12: **else**
13: Calculate $\mathbf{P}$ by Eq. (17).
14: **return** $\mathbf{P}$ and $\mathbf{P}_y \forall y \in Y$.
15: **end if**
16: **end if**

is computed as

$$\bar{A}_y^{w+1} = A_y^w \mathscr{P}_y^w + \hat{A}_y^w P_y^w, \tag{26}$$

where $\hat{A}_y^w$ is the equivalent Poisson arrival rate for the wavelength blocking sublayer and is derived from Eq. (14) at the proper instant, still in Step 4 (see Algorithm 2). Then, we update the probabilities and arrival rates for layers 2 to W in the same way. After passing the last layer, if the overall blocking has converged, the results are returned; otherwise, we return to Step 1 and iterate again from the first layer.

To illustrate the flow of the computation, we consider a network with three wavelengths, or $W = 3$, as an example. For each incoming call for source–destination pair $y \in Y$, the initialization Step 2 in Algorithm 2 computes $P_y^1, A_y^1, P_y^2, A_y^2, P_y^3, A_y^3$ from the first layer to the last layer. Then the QoT blocking sublayer computes $\mathscr{P}_y^1$ in Step 3. The wavelength blocking sublayer then takes this QoT BP and incorporates it into a revised $\bar{A}_y^2, \bar{V}_y^2, \bar{Z}_y^2$ in Step 4 in Algorithm 2. Step 2 in Algorithm 2 now reinitializes $P_y^2, A_y^2, P_y^3, A_y^3$ based on the updated overflow traffic statistics. Subsequently, the QoT blocking sublayer computes $\mathscr{P}_y^2$. Then revised $\bar{A}_y^3, \bar{V}_y^3, \bar{Z}_y^3$ are computed. The algorithm proceeds to compute $\mathscr{P}_y^1 \rightarrow \bar{A}_y^2, \bar{V}_y^2, \bar{Z}_y^2 \rightarrow \mathscr{P}_y^2 \rightarrow \bar{A}_y^3, \bar{V}_y^3, \bar{Z}_y^3 \rightarrow P_y^3, A_y^3 \rightarrow \mathscr{P}_y^3 \rightarrow \mathbf{P}_y$. This entire process constitutes one iteration of the algorithm, and is repeated until convergence is achieved. The main computational expense was found to lie in the derivation of $\mathscr{P}_y^w$, which is performed once per path, per wavelength, and per iteration.

V. Extensions

Our analytical model is flexible and can be extended to evaluate the performance of other scenarios. In this section, we first illustrate how to compute the BP for QoT-guaranteed RWA and then describe how to evaluate the BP for FFwO WA. These two extensions are further discussed in Section VI and validated for various networks.

A. Total BP for QoT-Guaranteed RWA

As shown in Fig. 1, the only difference between QoT-aware and QoT-guaranteed algorithms is that for QoT-guaranteed a part of the traffic is blocked out of the flow in each layer. The rate of the exiting flow is estimated by

$$\mathbb{A}_y^w = A_y \mathscr{P}_y^w (1 - P_y^w), \tag{27}$$

and the overflow traffic $\bar{A}_y^{w+1}$ for layer $w+1$ has to exclude the exiting flow and is computed as

$$\bar{A}_y^{w+1} = A_y^w \mathscr{P}_y^w P_y^w + \hat{A}_y^w P_y^w. \tag{28}$$

Thus, the total path BP $\mathbf{P}_y$ can be computed using

$$\mathbf{P}_y = \frac{\bar{A}_y^{W+1} + \sum_{w=1}^{W} \mathbb{A}_y^w}{\Phi_y}. \tag{29}$$

The total network BP in the network is given by

$$\mathbf{P} = \frac{\sum_{y \in Y} \Phi_y \mathbf{P}_y}{\sum_{y \in Y} \Phi_y}. \tag{30}$$

The algorithm (Algorithm 3) to compute the total BP for QoT-guaranteed RWA is similar to Algorithm 2, except that in Step 4, where the overflow traffic rate $\bar{A}_y^{w+1}$ is computed by Eq. (28), $\mathbb{A}_y^w$ has to be deducted from the overflow traffic to the next layer. In Step 9, the total path BP $\mathbf{P}_y$ is computed using Eq. (29), and in Step 13, the total BP $\mathbf{P}$ is derived using Eq. (30).

B. Impact of Static Wavelength Ordering

In [5,8], several wavelength ordering techniques are proposed to reduce crosstalk and hence reduce QoT blocking. Here we extend our analytical model to FFwO WA using the static wavelength ordering, as in [8]. The conventional FF wavelength assignment algorithm becomes the FFwO algorithm by picking the next candidate wavelength from the ordered list of wavelengths instead of sequentially, as is typically done. FFwO attempts to use wavelengths that are as spectrally separated as possible to avoid adjacent wavelength self-crosstalk. For example, instead of using wavelengths in the sequence $\{1,2,3,4,5\}$ in FF WA, FFwO picks wavelengths in the order $\{1,5,2,4,3\}$. Then, the more frequently used wavelengths with lower indices have less crosstalk impact on each other because the crosstalk power level is wavelength-dependent, with crosstalk from immediately adjacent wavelengths being

Algorithm 3 Algorithm to compute the total blocking for QoT-guaranteed RWA from wavelength $w = 1$ to W given $\bar{A}_y^1 = \Phi_y$, $\bar{V}_y^1 = \Phi_y$, and $\bar{Z}_y^1 = 1 \forall y \in Y$. Set $\mathbf{P}'_y = P_y$.

1: Set $w = 1$.
2: Wavelength blocking sublayer: $\forall y \in Y$, use Algorithm 1 to compute $P_y^{w'}$ and $A_y^{w'}$ for $w' = w$ to W.
3: QoT blocking sublayer: $\forall y \in Y$, compute $\mathscr{P}_y^w$ by Eqs. (22) and (24).
4: Wavelength blocking sublayer: $\forall y \in Y$, recalculate arrival rate $\bar{A}_y^w$ using Eq. (25); obtain $\bar{V}_y^w$, and $\bar{Z}_y^w$ by Eqs. (10) and (11); recalculate P_y^w using Eq. (8); use Eq. (14) to obtain $\hat{A}_y^w$; calculate $\bar{A}_y^{w+1}$ from Eq. (28); update $\bar{V}_y^{w+1}$, and $\bar{Z}_y^{w+1} \forall y \in Y$ by Eqs. (10) and (11).
5: Set $w = w + 1$.
6: **if** $w \le W$ **then**
7: Go to Step 2.
8: **else**
9: Calculate $\mathbf{P}_y$ by Eq. (29).
10: **if** $\exists y \in Y$ such that $\frac{|\mathbf{P}_y - \mathbf{P}'_y|}{\mathbf{P}_y} > \epsilon$ **then**
11: $\mathbf{P}'_y = \mathbf{P}_y$. Go to Step 1.
12: **else**
13: Calculate $\mathbf{P}$ by Eq. (30).
14: **return** $\mathbf{P}$ and $\mathbf{P}_y \forall y \in Y$.
15: **end if**
16: **end if**

more powerful than crosstalk from those separated by one or more wavelengths [8]. Note that we assume only adjacent wavelengths cause crosstalk in this paper. FFwO reduces crosstalk without sacrificing the desirable property of FF WA of using few wavelengths, which gives it a wavelength BP typically lower than that of the random-pick WA. For a QoT-guaranteed WA algorithm, wavelength ordering increases the chances that the considered wavelength has good QoT [8].

With the algorithm presented in [8], the BP for the FFwO WA is easily computed in the same way as for FF WA. Using the static ordering technique given in [8], we build a wavelength-layer index mapping table. The FFwO algorithm sends overflow traffic to the next layer, sequentially, as in the FF algorithm; what is different in FFwO is that these layers have been mapped to specific wavelengths, non-sequentially, so that adjacent wavelength crosstalk is minimized. Recall that self-crosstalk is induced only by adjacent wavelengths (as assumed in this analysis). The analysis described above can be directly applied to the FFwO algorithm by creating blocking event matrices $\xi_i^w[y]$ with rows containing wavelengths that correspond to adjacent layers, instead of $w-2, w-1, w, w+1, w+2$. Thus the overflow rates are the same as for the FF WA technique, only the calculation of the blocking events changes, since the channels that cause crosstalk are not invoked in the same order.

VI. Numerical Examples and Validation by Simulations

In this section, the analytical technique described above is used to predict the BP for several all-optical network topologies; simulations are used to validate the results. We first compare the results of the analysis to the approximation given in Subsection IV.E for the four-node tandem network shown in Fig. 6. We then use the approximate method for two other larger topologies: a seven-node ring network shown in Fig. 8 and the downsized NSF network shown in Fig. 9. A uniform load is assumed for both analysis and simulation. Unless otherwise stated, the physical parameters are given in Table I. Assume that PMD is negligible on the routes selected. The links in the topology are shown as bidirectional—each such link is actually two fibers, one in each direction. Simulation results are obtained by running more than 10^6 calls. We computed 95% confidence intervals for all data points, but they are not shown since they are all small compared to the scale of the plots. The QoT for the lightpaths being considered for (and affected by) each call is checked by counting the crosstalk terms occurring under the simulated network state and comparing the resulting BER to a threshold. In all analysis results, $\epsilon = 10^{-2}$. For all cases tried, computing the analytical results using the approximate method required computer running times orders of magnitude shorter than for simulation at this level of accuracy.

In all plots, the lines marked with circles are the results from simulation, and the lines marked with crosses are the results from analysis. We also plot the results without considering any physical impairments, where only the wavelength blocking is counted (as in [17]) for the seven-node ring and the NSF networks, marked with dotted lines, to show the accuracy of the wavelength BP model we used. Results for QoT-aware WA algorithms are plotted using solid lines and results for QoT-guaranteed WA algorithms are plotted using dash-dot lines. We analyze networks using a small number of wavelengths, $W = 5$ in the tandem network and the ring network and $W = 6$ and 16 in the NSF network, because the

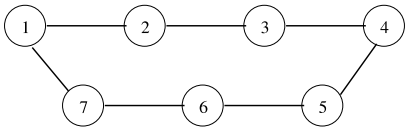

Fig. 8. Topology of the seven-node ring network used for analysis and simulation. Each link is 75 km long.

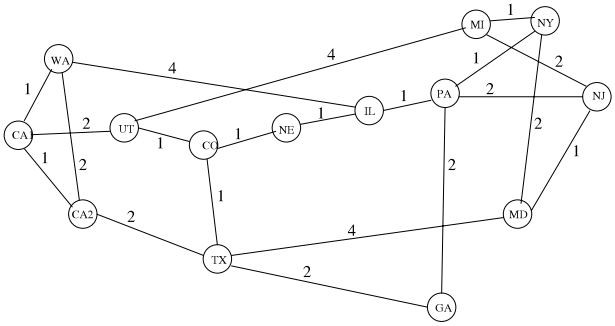

Fig. 9. Topology of a downsized version of the NSF network with 14 nodes and 21 bidirectional links, using link lengths 1/10 of their original size. The numbers on the links represent the number of spans along the link. Each span is around 75 km long.

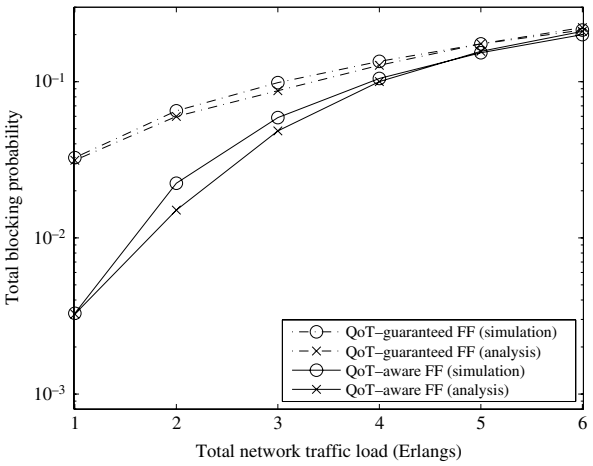

Fig. 10. FF WA BP computed using the accurate analysis and simulation for the four-node tandem network, $W = 5$. The data rate is 10 Gb/s, uncoded.

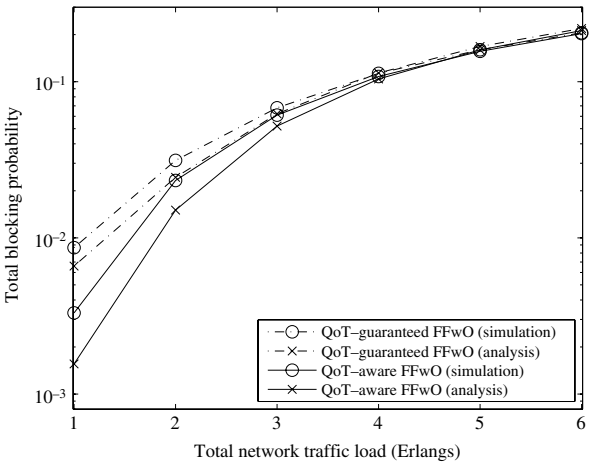

Fig. 11. FFwO WA BP computed using the accurate analysis and simulation for the four-node tandem network, $W = 5$. The data rate is 10 Gb/s, uncoded.

wavelength blocking model we use based on [17] is accurate only for the first few layers. As better analytical predictions for the wavelength BP in each layer are found, our approach can be directly meshed with them so that networks with large wavelength capacity can be studied.

A. Four-Node Tandem Network

Because the four-node tandem network is a symmetric network, we only consider unidirectional traffic, which has the same performance as the bidirectional case. The routing table used (including $N_{\max}$) is the same as in Table II.

1) Performance of FF and FFwO WAs: By using Algorithms 2 and 3 we obtain estimates of the BP for QoT-aware FF WA and QoT-guaranteed FF WA, as shown in Fig. 10. In medium and heavy traffic cases, the analytical results for the QoT-aware FF WA and QoT-guaranteed FF WA are close to the simulation results. When the traffic decreases, the analysis slightly underestimates the BP compared with the simulation result. Fredericks and Hayward's approximation [28] given in Eq. (14) accounts for the non-Poisson overflow, yet it underestimates the flow in each layer and leads to inaccuracy. For the QoT-guaranteed case, our algorithms remain accurate throughout the range of loads, where the BP is dominated by QoT blocking, and hence our calculation of QoT blocking is accurate. The flows are first blocked by the QoT constraint, and then blocked by the wavelength continuity constraint; thus an underestimation of wavelength BP may only slightly harm the results. In low traffic cases, the QoT BP is also dominant for QoT-aware WA; thus the flow rate is still quite close to the actual traffic. The analysis correctly predicts that QoT-aware WA is better at rejecting transmission impairment than QoT-guaranteed WA, yet some degradation remains.

For FFwO WA, the static ordering technique proposed in [8] is employed; the ordering table for five wavelengths is $\{1,5,2,4,3\}$. The performance is shown in Fig. 11. The analytical model correctly shows the improvement gained by using FFwO instead of FF in QoT-guaranteed cases. For completeness we also include QoT-aware FFwO, which provides no advantage compared to QoT-aware FF; it actually performs slightly worse than QoT-aware FF in some traffic levels because it uses all low crosstalk channels early, leaving no good quality channels for future calls. QoT-guaranteed algorithms do not iterate through all wavelengths; thus the ordering technique helps. If we add other physical layer impacts, such as neighbor-crosstalk, and consider the added complexity of estimating the QoT, the FFwO outperforms FF, which is shown in [8]. Again, we see that the results from the analysis are close to the simulation for various traffic loads and both algorithms, which validates our analytical model. Note that the analytical method is not as accurate for FFwO as for FF; the algorithm for FFwO must use wavelength blocking estimates for lower layers, which are themselves not as accurate because of Fredericks and Hayward's approximation.

2) Results of the Approximation Method: Because of the complexity of enumerating QoT blocking events, a computationally efficient approximation is proposed in Subsection IV.E to estimate the QoT BP. Because only some of the QoT blocking events are counted, i.e., those involving the spans that the chosen route traverses, the QoT blocking rate is underestimated. However, it causes Eq. (22) to increase, so the approximation gives an accurate estimate of the overall BPs nonetheless.

From Figs. 12 and 13, we conclude that the approximation closely estimates the simulated real BPs. The impact of QoT-aware and QoT-guaranteed RWAs is correctly approximated, for both FF and FFwO. Thus, in the following sections, we employ the approximation to obtain analysis results for networks larger than would be possible with the exact analysis.

B. Validation Via Simulation of Larger Networks

For the seven-node ring network, we model bidirectional links with five wavelengths in each direction. The same

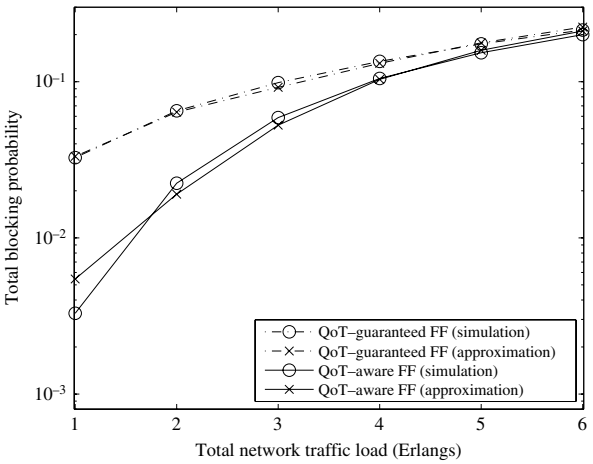

Fig. 12. FF WA BP computed using the approximate method and simulation for the four-node tandem network, $W = 5$. The data rate is 10 Gb/s, uncoded.

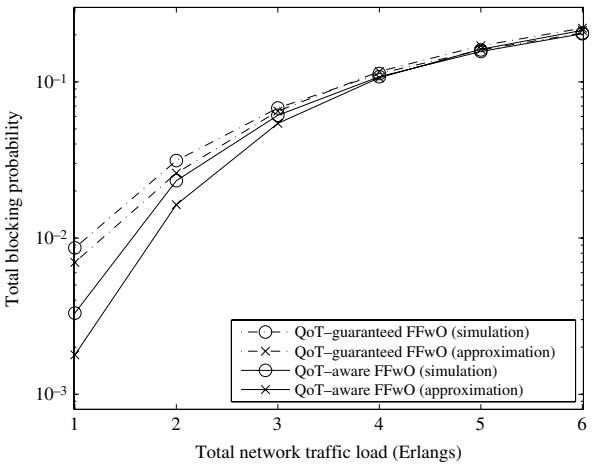

Fig. 13. FFwO WA BP computed using the approximate method and simulation for the four-node tandem network, $W = 5$. The data rate is 10 Gb/s, uncoded.

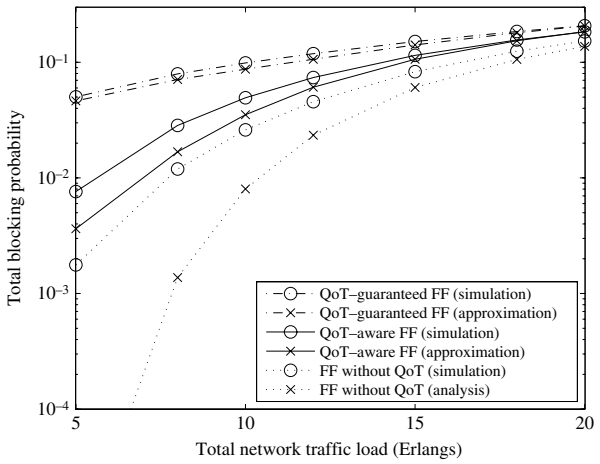

Fig. 14. FF WA BP computed using the approximate method and simulation for the seven-node ring network, $W = 5$. The data rate is 10 Gb/s, uncoded. In this and all subsequent plots, the bottom curves (FF without QoT) are based on the model in [17].

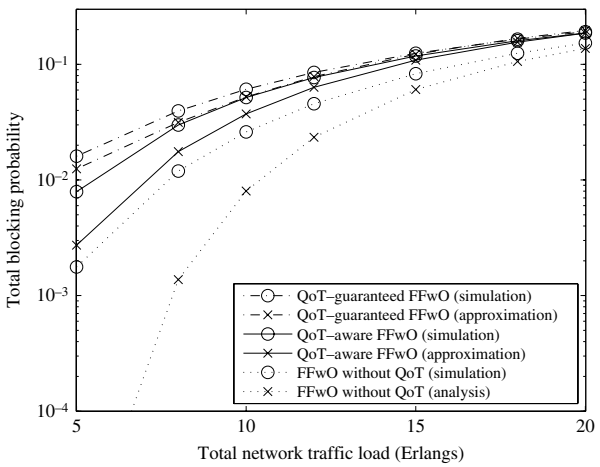

Fig. 15. FFwO WA BP computed using the approximate method and simulation for the seven-node ring network, $W = 5$. The data rate is 10 Gb/s, uncoded.

wavelength ordering table is used as for FFwO in the ring network. For the NSF network, we increase the number of wavelengths to six in each direction. In the next section we consider the accuracy of our model for a larger number of wavelengths. For FFwO WA, the ordering table for six wavelengths is $\{1,6,3,5,2,4\}$. Each link is divided into several spans, as noted in Fig. 9, and each span is equipped with a 20 dB gain EDFA to compensate for the fiber attenuation. The data rate is 10 Gb/s, and the BER threshold is 10^{-12}, assuming uncoded transmission. Other physical parameters are given in Table I. Because of the high level of noise, we limit the length of the all-optical lightpaths to three hops in the NSF network; longer paths require optical–electro-optical (OEO) or optical 3-R regeneration to restore the QoT and are not considered here. Note that the intermediate ROADM nodes are not counted as separate hops because ROADM nodes usually do not introduce much crosstalk.

The results for the ring network using FF WA and FFwO WA are shown in Figs. 14 and 15, respectively. The results for FF WA and FFwO WA in the NSF network are shown in Figs. 16 and 17, respectively. Here, we also plot the results without considering any physical impairments, where only the wavelength blocking is counted (as in [17]), marked with dotted lines. Note that the wavelength blocking estimates from [17] (labeled "without QoT") become less accurate as the load decreases. In low traffic loads, the underestimation of wavelength blocking causes the BPs in the analysis to be lower than the simulation result for both algorithms. Our QoT model can still estimate the QoT BP with a high degree of accuracy and so the overall network BP is more accurate than the cases without QoT blocking. In medium and high traffic loads, the performance difference decreases. In both networks, our analytical results predict the behavior of QoT-aware and QoT-guaranteed algorithms accurately for both FF WA and FFwO WA.

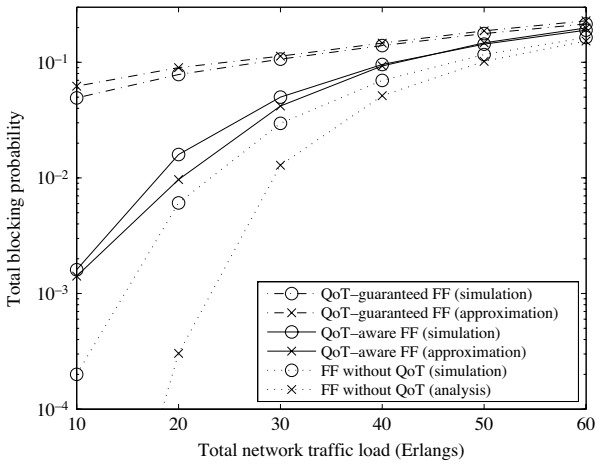

Fig. 16. FF WA BP computed using the approximate method and simulation for the scaled NSF network, $W = 6$. The data rate is 10 Gb/s, uncoded.

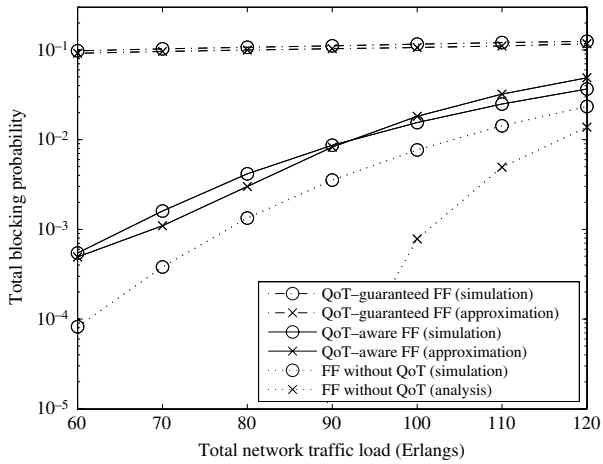

Fig. 18. FF WA BP computed using the approximate method and simulation for the scaled NSF network, $W = 16$. The data rate is 40 Gb/s, coded.

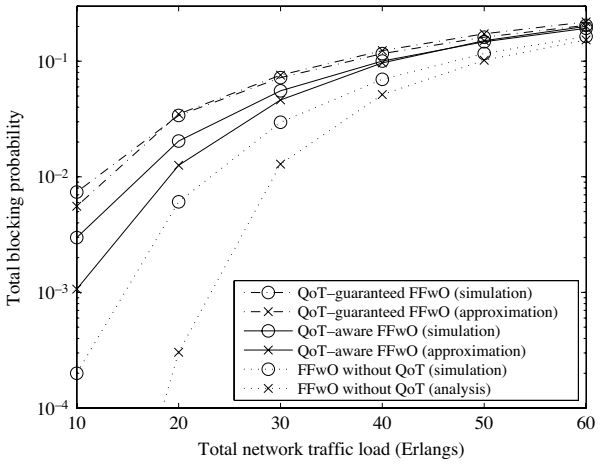

Fig. 17. FFwO WA BP computed using the approximate method and simulation for the scaled NSF network, $W = 6$. The data rate is 10 Gb/s, uncoded.

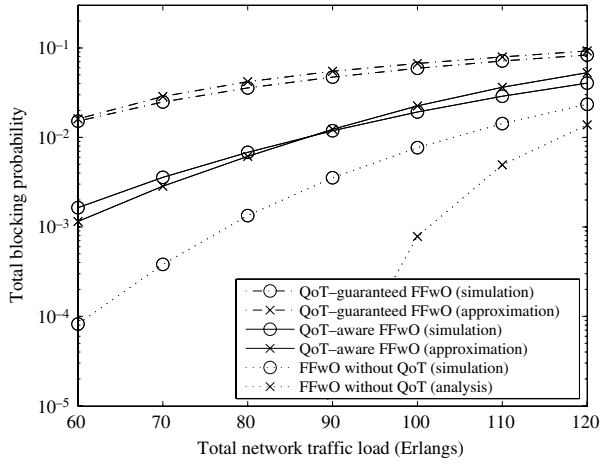

Fig. 19. FFwO WA BP computed using the approximate method and simulation for the scaled NSF network, $W = 16$. The data rate is 40 Gb/s, coded.

C. Results for a Larger Number of Wavelengths

To further investigate our model, we run simulation and analysis for a 16 wavelengths case ($W = 16$) for a data rate of 40 Gb/s in the 14-node NSF network. In practical systems, forward error coding (FEC) is usually used to improve the network performance. Also note that in 40 Gb/s systems, other impairments, such as PMD and nonlinear crosstalk, are no longer negligible; thus a certain performance margin should be reserved. Thus, we set the Q factor threshold to $Q = 4.25$, which corresponds to a pre-FEC BER of 10^{-5} or post-FEC BER of 10^{-15}, using generic forward error correction (GFEC) or enhanced forward error correction (EFEC) provided by ITU-T G.709 [29]. For FFwO WA, the ordering table for sixteen wavelengths is $\{1,16,8,12,4,6,10,14,2,15,3,13,5,11,7,9\}$. Unless otherwise stated, the notions and assumptions are the same as those in previous subsections.

The results for FF WA and FFwO WA are shown in Figs. 18 and 19, respectively. In all traffic loads, our analytical model is accurate and correctly estimates the network BP as compared to simulation. The analytical model also correctly predicts the behavior for various extensions, such as QoT-aware, QoT-guaranteed, FF WA, and FFwO WA algorithms. The accuracy when $W = 16$ is slightly better than when $W = 6$. For $W = 16$, QoT BP is a more important component in the total network BP compared with the $W = 6$ case. Our analytical model can accurately compute the QoT BP; thus the overall network BP for $W = 16$ is more accurate than that for $W = 6$.

When W is even larger, the underestimation of the wavelength BP causes the analytical model to mismatch the simulation, especially for the QoT-aware algorithm. The analytical model in this paper needs a higher level of accuracy from the wavelength BP model to correctly predict the network performance.

On our computing platforms,[2] the simulation on average requires 5 to 12 h (depending on the number of wavelengths and the traffic load) to handle 10^6 calls when QoT-aware WA is used, and around 30% less time when QoT-guaranteed WA is used. Note that the simulation running time is proportionate to the number of calls simulated. The running time of the analytical model is independent of the number of calls generated. Our analytical model requires 3 to 20 min (depending on the number of wavelengths and the traffic load) to perform the computation. In all cases, the analytical model is tens of times faster than the simulation.

VII. Conclusions

In this paper, we present an analytical technique to compute the total BP in WRONs impaired by self-crosstalk, ASE noise, thermal noise, and shot noise. The proposed model is the first of its kind to allow the evaluation of FF WA with QoT constraints. Our analytical model accurately predicts the blocking probabilities as validated by simulations. Moreover, our framework is easily extended to evaluate other algorithms; in particular, we employ it to evaluate QoT-guaranteed and FFwO WAs.

The performance is evaluated in three networks with different topologies, where the analysis results are shown to match the simulation. The discrepancy is due to approximations in the computation of the wavelength BP and not the computation of the QoT BP.

Heterogeneous networks can be studied and different levels of degradation can be considered for each path. We demonstrate the flexibility of our approach by incorporating different numbers of spans in the NSF network example. The technique can be generalized to study networks subject to other sources of QoT degradation, such as non-adjacent wavelength crosstalk, four wave mixing, or self- and cross-phase modulation. Our approximation works well, but for more complex and larger networks, a more sophisticated network separation algorithm may be needed.

Another possible extension is to evaluate RP WA using our approach. In conventional RP WA, all wavelengths are statistically identical. However, with the QoT constraint, wavelengths are no longer identical because of different numbers of QoT blocking events. We can roughly assume that all wavelengths are identical and use Algorithms 2 and 3 to estimate BPs for QoT-aware and QoT-guaranteed RP RWAs. Finding an accurate approximation of the BP for an RP WA with QoT constraints is still an open problem. These are opportunities for future study.

Acknowledgments

This work was supported by the National Science Foundation (NSF) under grants CNS-0520060, CNS-0519911, and CNS-0915795. This paper was presented in part at IEEE INFOCOM, Rio De Janeiro, Brazil, April 2009.

[2] We used several computers with Intel CPUs ranging from 2 to 2.4 GHz, with 2G or 3G of memory, and either WinXP or Win7 operating system.

References

[1] R. Martinez, C. Pinart, F. Cugini, N. Andriolli, L. Valcarenghi, P. Castoldi, L. Wosinska, J. Comellas, and G. Junyent, "Challenges and requirements for introducing impairment-awareness into the management and control planes of ASON/GMPLS WDM networks," *IEEE Commun. Mag.*, vol. 44, no. 12, pp. 76–85, Dec. 2006.

[2] J. Berthold, A. Saleh, L. Blair, and J. Simmons, "Optical networking: past, present, and future," *J. Lightwave Technol.*, vol. 26, no. 9, pp. 1104–1118, May 2008.

[3] T. Deng, S. Subramaniam, and J. Xu, "Crosstalk-aware wavelength assignment in dynamic wavelength-routed optical networks," in *Proc. Broadnets*, San Jose, CA, USA, Oct. 2004, pp. 140–149.

[4] I. Tomkos, D. Vogiatzis, C. Mas, I. Zacharopoulos, A. Tzanakaki, and E. Varvarigos, "Performance engineering of metropolitan area optical networks through impairment constraint routing," *IEEE Commun. Mag.*, vol. 42, no. 8, pp. S40–S47, Aug. 2004.

[5] J. He, M. Brandt-Pearce, Y. Pointurier, and S. Subramaniam, "Adaptive wavelength assignment using wavelength spectrum separation for distributed optical networks," in *Proc. IEEE Int. Conf. on Communications (ICC)*, Glasgow, UK, June 2007, pp. 2406–2411.

[6] S. Pachnicke, T. Paschenda, and P. Krummrich, "Assessment of a constraint based routing algorithm for translucent 10 Gbits/s DWDM networks considering fiber nonlinearities," *J. Opt. Netw.*, vol. 7, no. 4, pp. 365–377, Apr. 2008.

[7] G. Pavani, L. Zuliani, H. Waldman, and M. Magalhaes, "Distributed approaches for impairment-aware routing and wavelength assignment algorithms in GMPLS networks," *Comput. Netw.*, vol. 52, no. 10, pp. 1905–1915, July 2008.

[8] J. He, M. Brandt-Pearce, and S. Subramaniam, "QoS-aware wavelength assignment with BER and latency constraints for all-optical networks," *J. Lightwave Technol.*, vol. 27, pp. 462–474, Mar. 2009.

[9] S. Azodolmolky, M. Klinkowski, E. Marin, D. Careglio, J. Pareta, and I. Tomkos, "A survey on physical layer impairments aware routing and wavelength assignment algorithms in optical networks," *Comput. Netw.*, vol. 53, no. 7, pp. 926–944, 2009.

[10] S. Azodolmolky, Y. Pointurier, M. Angelou, J. Solé Pareta, and I. Tomkos, "Routing and wavelength assignment for transparent optical networks with QoT estimation inaccuracies," in *Proc. IEEE/OSA Optical Fiber Communication Conf. (OFC)*, San Diego, CA, USA, Mar. 2010, pp. 1–3.

[11] A. Birman and A. Kershenbaum, "Routing and wavelength assignment methods in single-hop all-optical networks with blocking," in *Proc. INFOCOM*, Boston, MA, USA, Apr. 1995, vol. 2, pp. 431–438.

[12] Y. Zhu, G. Rouskas, and H. Perros, "A path decomposition approach for computing blocking probabilities in wavelength-routing networks," *IEEE/ACM Trans. Netw.*, vol. 8, pp. 747–762, Dec. 2000.

[13] A. Sridharan and K. Sivarajan, "Blocking in all-optical networks," *IEEE/ACM Trans. Netw.*, vol. 12, pp. 384–397, Apr. 2004.

[14] C. Xin, C. Qiao, and S. Dixit, "Analysis of single-hop traffic grooming in mesh WDM optical networks," *Proc. SPIE*, vol. 5285, pp. 91–101, 2003.

[15] H. Waldman, D. R. Campelo, and J. Raul C Almeida, "A new analytical approach for the estimation of blocking probabilities in wavelength-routing networks," *SPIE*, vol. 5285, pp. 324–335, 2003.

[16] H. Harai, M. Murata, and H. Miyahara, "Performance analysis of wavelength assignment policies in all-optical networks with limited-range wavelength conversion," *IEEE J. Sel. Areas Commun.*, vol. 16, pp. 1051–1060, Sept. 1998.

[17] A. Alyatama, "Wavelength decomposition approach for computing blocking probabilities in WDM optical networks without wavelength conversions," *Comput. Netw.*, vol. 49, pp. 727–742, Dec. 2005.

[18] Y. Pointurier, M. Brandt-Pearce, and S. Subramaniam, "Analysis of blocking probability in noise and crosstalk impaired in all-optical networks," *J. Opt. Commun. Netw.*, vol. 1, pp. 543–554, Nov. 2009.

[19] B. Mukherjee, Y. Huang, and J. Heritage, "Impairment-aware routing in wavelength-routed optical networks," in *IEEE LEOS 2004*, 7–11 Nov. 2004, vol. 1, pp. 428–429.

[20] L. Eldada, "Optical add/drop multiplexing architecture for metro area networks," *SPIE Newsroom*, Jan. 2008.

[21] G. Agrawal, *Fiber-Optic Communication Systems*, 3rd ed. Wiley, New York, NY, USA, 2002.

[22] X. Ma and G.-S. Kuo, "Optical switching technology comparison: optical MEMS vs. other technologies," *IEEE Commun. Mag.*, vol. 41, no. 11, pp. S16–S23, Nov. 2003.

[23] H. Takahashi, K. Oda, and H. Toba, "Impact of crosstalk in an arrayed-waveguide multiplexer on $N \times N$ optical interconnection," *J. Lightwave Technol.*, vol. 14, pp. 1097–1105, June 1996.

[24] J. He, M. Brandt-Pearce, and S. Subramaniam, "Optimal RWA for static traffic in transmission-impaired wavelength-routed networks," *IEEE Commun. Lett.*, vol. 12, pp. 694–695, Sept. 2008.

[25] C. R. Menyuk and A. Galtarossa, *Polarization Mode Dispersion*. Springer, 2005.

[26] F. P. Kelly, *Reversibility and Stochastic Networks*. Wiley, New York, NY, USA, 1979.

[27] C.-T. Lea and A. Alyatama, "Bandwidth quantization and states reduction in the broadband ISDN," *IEEE/ACM Trans. Netw.*, vol. 3, no. 3, pp. 352–360, June 1995.

[28] A. Girard, *Routing and Dimensioning in Circuit-Switched Networks*. Addison-Wesley, 1990.

[29] "Juniper networks router-integrated OTN" [Online]. Available: http://www.juniper.net/us/en/local/pdf/datasheets/1000263-en.pdf.

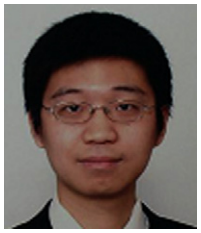

Jun He received his Ph.D. degree in electrical engineering from the University of Virginia in 2008. He is currently an Assistant Research Professor in the College of Optical Sciences at the University of Arizona. His research interests include optical communication, network modeling, network control and management, cross-layer issues in communication networks, and wireless sensor networks.

Dr. He has been on the program committees of several conferences including IEEE WCNC, IEEE ICC, and ICST GridNets. He currently serves on the editorial boards of Elsevier journal of *Computers and Electrical Engineering* and the *Journal of Networks*.

Maïté Brandt-Pearce received her B.S. in electrical engineering from Rice University in 1985. She completed an M.E.E. in 1989 and the Ph.D. in electrical engineering in 1993, both also from Rice University. She worked with Lockheed in support of NASA Johnson Space Center from 1985 until 1989. In 1993, Dr. Brandt-Pearce joined the Charles L. Brown Department of Electrical and Computer Engineering at the University of Virginia, where she is currently a full Professor. Dr. Brandt-Pearce's research interests lie in the mathematical and numerical characterization and optimization of communication systems with multiple simultaneous components from different sources. This interest has found applications in a variety of research projects including multiuser demodulation and detection, study of nonlinear effects on fiber-optic multichannel communications, optical networks subject to physical layer degradations, free-space optical multiuser communications, and radar signal processing and tracking of multiple targets. Dr. Brandt-Pearce is the recipient of an NSF CAREER Award, an NSF RIA, and an ORAU Junior Faculty Enhancement Award. She is a co-recipient of Best Paper Awards at the ICC 2006 Symposium on Optical Systems and Networks. She is a member of Tau Beta Pi, Eta Kappa Nu, and a senior member of the IEEE.

Suresh Subramaniam (S'95-M'97-SM'07) received the Ph.D. degree in electrical engineering from the University of Washington, Seattle, in 1997. He is a Professor in the Department of Electrical and Computer Engineering at the George Washington University, Washington, DC. His research interests are in the architectural, algorithmic, and performance aspects of communication networks, with particular emphasis on optical and wireless ad hoc networks.

Dr. Subramaniam is a co-editor of the books *Optical WDM Networks—Principles and Practice* and *Emerging Optical Network Technologies: Architectures, Protocols, and Performance*. He has been on the program committees of several conferences including Infocom, ICC, Globecom, OFC, and Broadnets, and served as TPC Co-Chair for the optical networks symposia at Globecom 2006 and ICC 2007. He currently serves on the editorial boards of the *IEEE/ACM Transactions on Networking*, *Optical Switching and Networking*, and KICS *Journal of Communications and Networks*. He is a co-recipient of Best Paper Awards at the ICC 2006 Symposium on Optical Systems and Networks, and at the 1997 SPIE Conference on All-Optical Communication Systems.